# Phosphorylation of Serine 11 and Serine 92 as New Positive Regulators of Human Snail1 Function: Potential Involvement of Casein Kinase-2 and the cAMP-activated Kinase Protein Kinase A

**Matthew Reid MacPherson,\*†‡ Patricia Molina,\*† Serhiy Souchelnytskyi,§ Christer Wernstedt,‖ Jorge Martin-Pérez,\* Francisco Portillo,\* and Amparo Cano\***

\*Departamento de Bioquímica, UAM, Instituto de Investigaciones Biomédicas "Alberto Sols," CSIC-UAM, 28029 Madrid, Spain; §Karolinska Biomics Center, Department of Oncology-Pathology, Karolinska Institutet, SE-17176, Stockholm, Sweden; and ‖Ludwig Institute for Cancer Research, Uppsala S-751 24, Sweden

Snail1 is a major factor for epithelial-mesenchymal transition (EMT), an important event in tumor metastasis and in other pathologies. Snail1 is tightly regulated at transcriptional and posttranscriptional levels. Control of Snail1 protein stability and nuclear export by GSK3$\beta$ phosphorylation is important for Snail1 functionality. Stabilization mechanisms independent of GSK3$\beta$ have also been reported, including interaction with LOXL2 or regulation of the COP9 signalosome by inflammatory signals. To get further insights into the role of Snail1 phosphorylation, we have performed an in-depth analysis of in vivo human Snail1 phosphorylation combined with mutational studies. We identify new phosphorylation sites at serines 11, 82, and 92 and confirmed previously suggested phosphorylations at serine 104 and 107. Serines 11 and 92 participate in the control of Snail1 stability and positively regulate Snail1 repressive function and its interaction with mSin3A corepressor. Furthermore, serines 11 and 92 are required for Snail1-mediated EMT and cell viability, respectively. PKA and CK2 have been characterized as the main kinases responsible for in vitro Snail1 phosphorylation at serine 11 and 92, respectively. These results highlight serines 11 and 92 as new players in Snail1 regulation and suggest the participation of CK2 and PKA in the modulation of Snail1 functionality.

## INTRODUCTION

Epithelial-mesenchymal transition (EMT) is a process whereby cells lose cell–cell interactions and other epithelial properties while acquiring a more migratory and mesenchymal phenotype. EMT occurs at several stages of early development and an EMT-like process is thought to occur during tumor progression (Thiery, 2002; Gupta and Massagué, 2006; Moreno-Bueno et al., 2008; Yang and Weinberg, 2008). A hallmark of EMTs is the functional loss of E-cadherin (CDH1) which mediates cell-cell interactions. Snail1 is one of a family of transcription factors shown to repress transcription of the CDH1 gene (Cano et al., 2000; Batlle et al., 2000)

† These authors contributed equally to this work.

‡ Present address: Division of Pathology and Neuroscience, Ninewells Hospital and Medical School, University of Dundee, Dundee DD1 9SY, United Kingdom.

Address correspondence to: Francisco Portillo (fportillo@iib.uam.es) or Amparo Cano (acano@iib.uam.es).

Abbreviations used: CK2, casein kinase-2; DB, destruction box; GSK3$\beta$, glycogen synthase kinase 3-beta; GST, gluthatione S-transferase; NES, nuclear export signal; PAK1, p21-activated kinase; PKA, protein kinase A (cAMP-activated kinase); SNAG, SNAIL and Gfi conserved domain; SRD, serine-rich domain.

and has been shown to be crucial to development in mice, because Snail1 knockout mutants die at gastrulation (Carver et al., 2001). Snail1 also regulates the expression of different target genes involved in EMT and other functions, such as cell survival (reviewed in Barrallo-Gimeno and Nieto, 2005). Importantly, Snail1 has been shown to be up-regulated in various tumor types (reviewed in Peinado et al., 2007) and has more recently been observed expressed at the tumor stromal interface (Francí et al., 2006, 2009).

To date, several studies have examined the posttranslational modifications that control Snail1 cell function. Snail1 consists of four C-terminal DNA-binding zinc fingers and a regulatory region spanning amino acids 1–150 (Sefton et al., 1998), comprising an N-terminal SNAG (SNAIL and Gfi conserved) domain (1–9 amino acids) important for corepressor interaction (Hemavathy et al., 2000; Peinado et al., 2004), and the serine-rich domain (SRD), which appears to control the function of a short leucine-rich nuclear export sequence (NES) recognized by the CRM1 transporter (Domínguez et al., 2003; Zhou et al., 2004). Initial studies demonstrated that the SRD was important for subcellular localization and that mutation of all serines-to-alanine residues in that region resulted in cytoplasmic localization of Snail1 and consequent repressive dysfunction (Domínguez et al., 2003). Additionally, two separate investigations (Zhou et al., 2004; Yook et al., 2005) identified a short sequence in the SRD important for Snail1 posttranslational regulation. This short sequence is conserved in several proteins, including $\beta$-catenin and IK$\kappa$B, and is termed destruction

box (DB). The DB in the case of $\beta$-catenin contains two serines, the phosphorylation of which is critical for recognition and ubiquitination by the $\beta$-TrCP ubiquitin ligase (Nelson and Nusse, 2004). This leads to proteasomal degradation and thereby constitutes an important shared control mechanism for the government of several transcriptional regulators simultaneously. In Snail1 these serines lie at positions 96 and 100 (D$^{96}$SGKG$^{100}$SQPP), are evolutionary conserved, and are the target for the protein kinase glycogen synthase kinase 3-beta (GSK3$\beta$). Mutation of these serines to alanine leads to increased Snail1 stability (Zhou *et al.*, 2004). Yook *et al.* also identified two additional conserved serines (QPP$^{104}$SPP$^{107}$SPAP) as targets for the serine/threonine protein kinase GSK3$\beta$. Based on those results two models were proposed to explain the regulation of Snail1 by GSK3$\beta$. Yook *et al.* (2005) proposed that phosphorylation of serines 104 and 107 would prime GSK3$\beta$ phosphorylation of serines 96 and 100 in the DB, thus leading to ubiquitination and degradation of Snail1. In support of this model they found that GSK3$\beta$ was one of the components of a regulatory complex, including Axin2 that facilitates the shuttling of GSK3$\beta$ between nucleus and cytoplasm (Yook *et al.*, 2006). Zhou *et al.* (2004) proposed a slightly different model whereby nuclear GSK3$\beta$ phosphorylation of serines 107, 111, 115, and 119 prompts Snail1 nuclear export. Cytoplasmic Snail1 is then phosphorylated at serines 96 and 100 by GSK3$\beta$ promoting ubiquitination and degradation. An additional proposed modulator of Snail1 was p21-activated kinase (PAK1), which may phosphorylate Snail1 at serine 246 (TF$^{246}$SRM) to favor its nuclear localization (Yang *et al.*, 2005). This serine is conserved in all the members of the Snail family and is located within the C-terminal zinc finger domain (Manzanares *et al.*, 2001; Nieto, 2002). Posttranslational regulation of Snail1 stability by GSK3$\beta$-independent mechanisms has also been reported, including stabilization by lysyl oxidase like-2 (LOXL2) interaction (Peinado *et al.*, 2005), mediated by TNF-$\alpha$/NF-$\kappa$B and COP9 signalosome (Wu *et al.*, 2009a), and cap-independent translational regulation by YB-1 factor (Evdokimova *et al.*, 2009). On the other hand, interaction between Snail and the F-box protein PpA has also been implicated in Snail2 stabilization (Vernon and Labonne, 2006).

The phosphorylation of Snail1 in previous studies has been analyzed by mutation of the serine residues or by alterations of the mobility shift in Western blots, but not by in vivo analysis of Snail1 phosphorylation sites. In the present study, we have performed a complete analysis of Snail1 phosphorylation in vivo to clarify and complement previous investigations. We have identified several new sites of phosphorylation (S11, S82, and S92) with regulatory implications in Snail1 functionality as well as confirming some of those previously described (S104 and S107). We also propose that, in addition to GSK3$\beta$, the ubiquitous serine/threonine protein kinase CK2 (casein kinase-2) and the cAMP-activated kinase PKA (protein kinase A) may play a role in Snail1 function and regulation.

## MATERIALS AND METHODS

### Generation of Plasmids and Expression Vectors

The pcDNA3-HA plasmid containing human *SNAIL1* cDNA described previously (Peinado *et al.*, 2005) has been used as a template for site-directed mutagenesis. Site-directed mutagenesis was performed as described (Zheng *et al.*, 2004). After mutagenesis, the entire *SNAIL1-HA* was sequenced to verify that only the nucleotide changes introduced by the mutagenic oligonucleotide were obtained. Vectors for expression of Snail1 fused to the GST (glutathione *S*-transferase) protein were generated through PCR amplification of human Snail1 coding region from pcDNA3-Snail1-HA plasmid using oligonucleo-

tides 5'-gcggatcccatgccgcgctctttc-3' and 5'-gcgaattcagcggggacatcctgagc-3' containing restriction sites for BamHI and EcoRI, respectively. The resulting product was digested and cloned into pGEX4T3 and sequenced to confirm identity. The mSin3A-myc-pcDNA3 expression vector was previously described (Peinado *et al.*, 2005).

### Cell Culture and Transfections

HEK293T and MDCK cells were maintained in DMEM medium supplemented with 10% fetal calf serum and antibiotics (100 $\mu$g/ml ampicillin, 32 $\mu$g/ml gentamicin, Sigma-Aldrich, St. Louis, MO). Stable and transient transfections were performed using Lipofectamine reagent (Invitrogen, Carlsbad, CA) according to manufacturer's instructions. For generation of stable clones MDCK cells ($1 \times 10^6$ cells) grown in P100 plates were transfected with the indicated Snail1-HA wild-type, mutant constructs, or control pcDNA3 construct (cytomegalovirus [CMV]) and grown in the presence of G418 (500 $\mu$g/ml) for 2–3 wk; individual colonies were then selected and grown individually. At least 10 independent clones were selected and characterized from each transfection with the pcDNA3-Snail1-HA mutants. Two independent clones were additionally selected from pcDNA3-Snail1-HA wild-type or control transfections and compared with similarly isolated clones from our previous studies (Peinado *et al.*, 2005).

### Yeast Two-Hybrid Screen

The two-hybrid screen was performed as previously described (Peinado *et al.*, 2005), using the Matchmaker system 3 (Clontech, Palo Alto, CA). The bait protein was the N-terminus of mouse Snail1 (residues 1-150). A fibroblast NIH3T3 library in pACT2 vector (Clontech) was used. Positive colonies were isolated based on their capacity to express the markers *ADE2, HIS3,* and *MEL1*.

### In Vivo Phosphorylation

Human embryonic kidney HEK293T cells were grown in 30-mm-diameter plates and transfected with pcDNA3-Snail1-HA wild-type or the indicated pcDNA3-Snail1-HA mutants. After 24–36 h, cells were washed three times with DMEM phosphate-free medium, supplemented with 10% fetal calf serum, and subsequently incubated in the same medium containing 1 mCi/ml [$^{32}$P]orthophosphate (Amersham, Piscataway, NJ) for 4 h. Cells were lysed with ice-cold RIPA buffer (0.1% SDS, 0.5% sodium deoxicholate, 1% NP-40, 150 mM NaCl, 50 mM Tris-HCl, pH 8.0) containing protease (2 $\mu$g/ml aprotinin, 1 $\mu$g/ml leupeptin, 1 mM PMSF) and phosphatase inhibitors (1 mM sodium vanadate, 10 mM sodium fluoride), the resulting lysate centrifuged at $14,000 \times g$ for 15 min, and the supernatant was incubated overnight at 4°C with 1 $\mu$g anti-HA and 25 $\mu$l of protein G-Sepharose (Amersham). Immunoprecipitates were collected and washed four times with ice-cold RIPA buffer. Precipitated proteins were resolved by SDS-PAGE and transferred to nitrocellulose membrane before exposure to x-ray film overnight to view radioactively labeled proteins.

### Phosphopeptide Mapping

Phosphopeptide mapping was performed as described (Boley *et al.*, 1991; Van Der Geer and Hunter, 1994). Briefly, phosphorylated Snail1 bands were excised from the membrane and blocked for 30 min in 0.5% polyvinylpirrolidon K30 (Sigma-Aldrich), 0.6% acetic acid at 37°C. After several washes with distilled water, bands were each incubated overnight in 50 mM NH$_4$HCO$_3$, pH 8.0, with 1 $\mu$g modified sequencing grade trypsin (Promega, Madison, WI) at 37°C. The solution containing eluted peptides was transferred to a fresh tube and the radioactivity measured to ensure efficient elution. The peptides were then frozen and dried by vacuum evaporation. They were then oxidized in performic acid for 1 h on ice in the dark. The oxidization was stopped through dilution in water, the solution was frozen, and vacuum evaporated. A further overnight digestion with trypsin was required to ensure efficient trypsin digestion. The peptides were then washed twice in water, with vacuum-evaporating in between, and then were resuspended in 200 $\mu$l electrophoresis running buffer (2.5% formic acid, 7.5% acetic acid, pH 1.9), centrifuged 15 min at $15,000 \times g$, to remove remaining insoluble material. The supernatant was then dried and resuspended in 10 $\mu$l electrophoresis running buffer and carefully spotted onto a $20 \times 20$-cm cellulose TLC plate (TLC plates cellulose were precoated, without fluorescent indicator and with layer thickness 0.1 mm; cat. no. 5716, Merck, Rahway, NJ). Electrophoresis was performed using HTLE-700 high-voltage electrophoresis apparatus (CBS Scientific, Del Mar, CA) for 30 min at 2000 V. The plates were then allowed to dry for a minimum of 6 h before chromatography. Separation of peptides by chromatography was performed for 14–16 h in isobutyric acid buffer (62.5% isobutyric acid, 3% acetic acid, 2% *n*-butanol, 5% pyridine). After drying for at least 6 h, the plates were exposed to phosphoimaging screen (Fujifilm, Tokyo, Japan). The results were observed using a Typhoon variable mode imager (GE Healthcare, Waukesha, WI) or Fuji FLA-3000 PhosphorImager (Fuji) and the images adjusted using Adobe Photoshop version 7.0 (San Jose, CA).

### Edmann Degradation

Phosphopeptides were eluted from the plates in pH 1.9 electrophoresis buffer and lyophilyzed. The fractions were then subjected to automated Edmann degradation. For Edmann degradation, phosphopeptides (40–500 cpm) were coupled to Sequelon-AA membranes (Millipore, Bedford, MA) according to the manufacturer's instructions and sequenced on an Applied Biosystems Gas Phase Sequencer model 470A (Foster City, CA). Released phenylthiohydantoin amino acid derivatives from each cycle were spotted onto TLC plates. The radioactivity in each spot was quantitated by exposure to a screen and scanning in a FLA-300 PhosphorImager (Fuji).

### In Vitro Kinase Assays

In vitro kinases assays were performed by incubation of 1 μg of GST-Snail1 fusion protein or GST alone with 10 U of the stated kinase in the supplied buffer, supplemented with 100 μM ATP and 1 μCi [γ-$^{32}$P]ATP. Reactions were left for 30 min at 30°C and stopped by addition of 2× Laemmli buffer. Proteins were resolved by 10% PAGE-SDS electrophoresis and transferred to nitrocellulose membranes, which were then exposed to x-ray film. Human recombinant CK2 holoenzyme and human PKA catalytic subunit were purchased from Calbiochem (Darmstadt, Germany; cat. no. 218701) and Sigma-Aldrich (cat. no. C8482), respectively.

### Coimmunoprecipitation and Western Blot Assays

Coimmunoprecipitation analyses were performed as described previously (Peinado *et al.,* 2004). Basically, HEK293T cells were transiently transfected with the indicated vectors for 48 h. Lysates were then obtained in immunoprecipitation buffer (50 mM Tris-HCl, pH 8.0, 150 mM NaCl, 5 mM EDTA, 0.5% NP-40) containing protease and phosphatase inhibitors (2 μg/ml aprotinin, 1 μg/ml leupeptin, 1 mM PMSF, 1 mM sodium vanadate, 10 mM sodium fluoride) and precleared with Sepharose G-beads. Supernatants were subjected to overnight incubation with anti-HA affinity matrix (Roche, Indianapolis, IN) or Sepharose G-beads coated with anti-rat IgG as immunoprecipitation control. Immunoprecipitates were resolved in 7.5–12% PAGE-SDS gels, transferred to membranes, and incubated with the indicated antibodies. Membranes were finally developed using ECL reagent following manufacturer's instructions (Amersham). Blots were incubated with rat anti-HA (Roche; 1:400), or anti-myc (Santa Cruz Biotechnology, Santa Cruz, CA; 1:200). For characterization studies, whole cell extracts were fractionated in SDS-PAGE gels and subjected to Western blot analyses with anti-E-cadherin, anti-HA, and anti-α-tubulin as described (Cano *et al.,* 2000; Peinado *et al.,* 2005). When indicated, MAb anti-Snail1 EC3 (1:100; Francí *et al.,* 2006) was used. The secondary antibodies used were HRP-coupled sheep anti-mouse (1:1000), goat anti-rabbit (1:4000; Amersham), or anti-rat (1:10,000; Pierce, Rockford, IL).

### Protein Stability

Snail1-HA wild-type or the indicated Snail1-HA mutant constructs were transiently transfected into HEK293T cells, and 24 h later cells were treated with 20 mM cycloheximide (Sigma-Aldrich) for the indicated time intervals. Cells were lysed in RIPA buffer, containing protease and phosphatase inhibitors (2 μg/ml aprotinin, 1 μg/ml leupeptin, 1 mM PMSF, 1 mM sodium vanadate, 10 mM sodium fluoride), and the expression of Snail1 was analyzed by Western blotting using anti-HA antibody (Roche) as above, using α-tubulin as loading control.

### Immunofluorescence Analysis

Immunofluorescence analysis for E-cadherin, vimentin, and Snail1-HA were performed on cells grown on glass coverslips and fixed in cold methanol as previously described (Cano *et al.,* 2000; Peinado *et al.,* 2005). The secondary antibodies used were anti-rat Alexa594 and anti-mouse Alexa488 (1:800; Molecular Probes, Eugene, OR). Preparations were visualized in a Nikon N90i microscope (Melville, NY) equipped with epifluorescence.

### Pulldown Assays

HEK293T cells transiently transfected with pcDNA-CK2α-HA were lysed in RIPA buffer after a 48-h expression period. Lysates were then incubated with 10 μg of recombinant GST-Snail1 or GST control protein coupled to 50 μl glutathione-Sepharose for 1 h at 4°C. The beads were then washed four times for 15 min each in 1 ml RIPA buffer containing 0.5 M NaCl and then resuspended in 2× Laemmli buffer. The samples were then boiled for 5 min before be analyzed in 10% PAGE-SDS gels to detect associated CK2α with anti-HA antibodies (Roche).

### E-Cadherin and Claudin 1 Promoter Analysis

The human and mouse *E-cadherin* promoters (−178 to +92 in both cases) fused to luciferase were used to determine the activity of the *E-cadherin* promoter as described previously (Peinado *et al.,* 2004, 2005). The human *claudin-1* promoter (−748 to +252) fused to luciferase was also used as previously described (Martinez-Estrada *et al.,* 2006). Cotransfections were carried out in the presence of the indicated amounts of Snail1-HA or

Snail1-HA mutant cDNAs, all cloned in the pcDNA3 vector. The amount of total transfected DNA was normalized with empty pcDNA3 vector. Luciferase and renilla activities were measured using the dual luciferase reporter assay kit (Promega) and normalized to the wild-type promoter activity in mock (pcDNA3) transfected cells, as previously described (Peinado *et al.,* 2004, 2005).

## RESULTS

### Snail1 Is Multiply Phosphorylated in Vivo

Although analysis of in vivo Snail1 phosphorylation had previously been carried out (Domínguez *et al.,* 2003), detailed analyses of specific sites had not. It had been demonstrated that the majority of Snail1 phosphorylation took place on serine residues and that although many sites resided within the serine rich domain, others lay outside this region. Therefore, to obtain additional information we undertook phosphopeptide mapping of in vivo phosphorylated human Snail1 after being transiently expressed in HEK293T cells.

Phosphorylated Snail1 appeared as one main band with further fainter bands also apparent in the parallel Western blot control, possibly due to partial degradation (Figure 1A). The main phosphorylated band was excised and subjected to trypsin digestion, and the resulting peptides separated in two-dimensions by electrophoresis and chromatography. The resultant phosphopeptide map showed a minimum of eight distinct phosphopeptides, suggesting several phosphorylation sites in Snail1 (Figure 1B).

Each phosphopeptide was extracted from the cellulose plate and subjected to Edmann's degradation with the resultant residues spotted on TLC cellulose plates (Figure 1C). This analysis indicated that phosphopeptide 1 was phosphorylated on the 3rd residue, phosphopeptides 2 and 4 on the 8th residue, phosphopeptide 3 on the 4$^{th}$ residue, and phosphopeptides 5 and 6 on the 6th and 9th residues (Figure 1C). Phosphopeptides 7 and 8 could not be sufficiently eluted to allow reliable sequencing (data not shown). This analysis suggested multiple possible phosphorylation sites (Figure 1D) when compared with the all potential predicted peptides produced by trypsin digest of Snail1 protein as shown in Figure 1E.

### Snail1 Is Phosphorylated In Vivo at Positions 11, 82, 92, 104, and 107

To confirm the specific phosphorylation sites in Snail1 for each possible phosphorylation site, serine-to-alanine mutants were generated by site directed mutagenesis of the appropriate residues. The resulting S-to-A mutants were compared with the wild-type Snail1 protein for differences in the in vivo phosphorylation pattern. The disappearance of a particular spot in the S-to-A mutant relative to wild type being taken as confirmation of serine phosphorylation at this site. For each of phosphopeptides 1–6, a corresponding S-to-A mutant was found lacking the corresponding phosphopeptide.

Peptide 1 represented phosphorylation at serine 11 of Snail1 (Figure 2B, cf. Figure 2A) adjacent to the SNAG domain (Figure 1E) and proximal to lysine residues thought to be involved in nuclear entry (Ko *et al.,* 2007).

Phosphopeptide 2 (Figure 1C) represented phosphorylation at serine 92 at the N-terminal of the SRD (Figure 2D). There appeared to be no additional phosphorylations on this peptide possibly expected at serine 96 (Figure 2D).

Phosphopeptide 3 represents phosphorylation at serine 82 at the N-terminal of the SRD (Figure 2C). Interestingly, phosphopeptide 3 is not detected in mutant S92A (Figure 2D), suggesting that the phosphorylation at serine 92 is

**Figure 1.** Snail1 is phosphorylated in vivo at several potential serine residues. In vivo phosphorylation of Snail1-HA was analyzed after transient transfection in HEK293T cells. (A) Autoradiography on immunoprecipitates obtained with anti-HA antibodies from HEK-293T transfected with Snail1-HA, labeled with $^{32}$P-orthophosphate (left); parallel Western blot analysis with anti-HA antibodies (right) of lysates from $^{32}$P-labeled cells. (B) Two-dimensional phosphopeptide analysis of immunoprecipitated $^{32}$P-Snail1-HA after typsin digestion. The main phosphopeptides detected are indicated by circles and numbered 1–8. (C) Edmann degradation analyses of the indicated Snail1-$^{32}$P-phosphopeptides. The amino acid position from the N-terminal of the different peptides is numbered from 1 to 10 above. (D) Hypothetical phosphorylated residues in the different identified phosphopeptides. (E) Top, the sequence of human Snail1 with the location of all potential trypsin peptides is indicated by arrows; a color code corresponding to the different regulatory/structural domains of Snail1, indicated in the lower diagram, is used. Red, potential phosphorylated residues in each peptide. SNAG Snail1, transrepressor domain; NES, nuclear export signal; the DNA-binding domain contains the four zinc finger region.
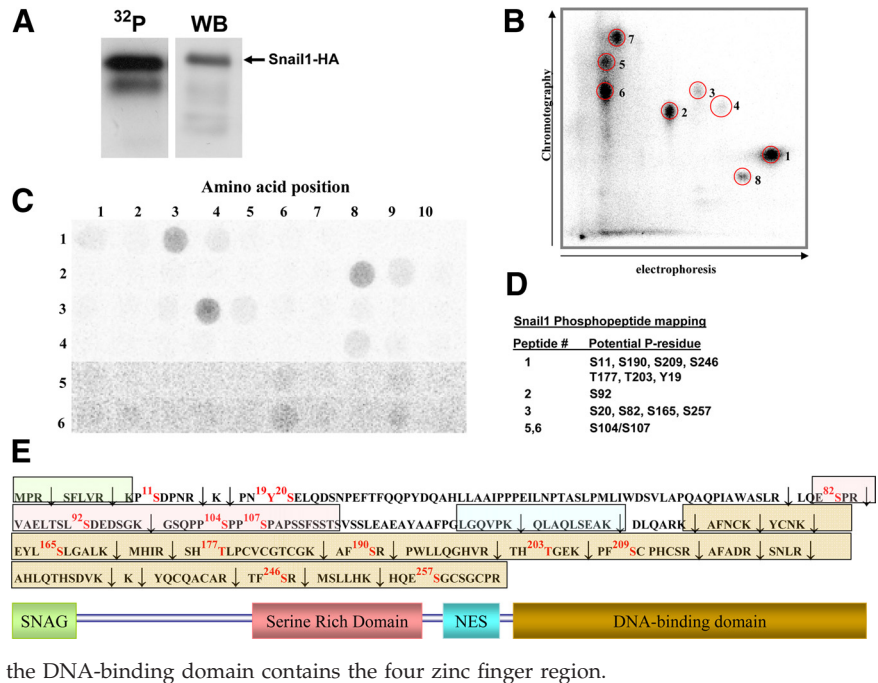


required for phosphorylation at serine 82. Phosphopeptide 4 was weakly detected in most Snail1-HA mutants, making its identification difficult. However, its Edmann's degradation pattern was similar to that of peptide 2 (Figure 1C), and its complete disappearance in S11A and S92A mutants suggests it may correspond to a miscut or other posttranslational modifications.

Phosphopeptides 5 and 6 both represent phosphorylations at serines 104 and 107 (Figure 2E). Indeed, there appear to be several peptide species with high hydrophobicity and low electrophoretic mobility. This group of phosphopeptides was poorly resolved in most of the analyzed mutants (see Figure 2, B–F), and these are thought to represent various modes of posttranslational modification of peptide 99-137, in particular affecting serine 104 and serine 107, because they disappear in the S104A/S107A mutants (Figure 2E). Peptide 99-137 exhibits no charge and a high hydrophobicity (aprox. 0.61), and phosphorylation of one to three serines in the peptide would have a very weak impact on migration in chromatography, due to the considerable length of the peptide.

Of note was the absence of peptides phosphorylated at serines 96 or 100, the two serines within the DB motif, proposed previously to be phosphorylated by GSK3$\beta$ (Zhou et al., 2004; Yook et al., 2005). One possible explanation may be that subsequent ubiquitination and degradation of phospho-serine 96/100 protein occurs so quickly as to prevent attainment of these phosphopeptides. Although not observed, it is important not to discount other possible phosphorylations within the SRD as the large size of this peptide and progressive weakness of signal obtained from Edmann's sequencing may have obscured further downstream phosphorylations occurring at serines 111, 115, and 119.

Interestingly, the triple mutation of serines 92, 104, and 107 almost completely ablated phosphopeptides expected to represent phosphorylation in the SRD (Figure 2F). Therefore, it appears that either further phosphorylation in this region does not occur or that such phosphorylations are principally dependent on phosphorylations of serines 92, 104, and 107.

It was previously reported that Snail1 is phosphorylated at serine 246 by PAK1 (Yang et al., 2005). However, we were unable to detect any potential phosphopeptide corresponding to TF$^{246}$SR, even under shorter electrophoretic run (to prevent the loss of high mobility peptides; Supplemental Figure S1). Furthermore, analysis of in vivo phosphorylation of S246A mutation did not reveal any change in its phosphorylation pattern compared with wild-type Snail1 (Supplemental Figure S2), suggesting that no phosphorylation occurs at serine 246 in our experimental system. It is possible, however, that there was insufficient PAK1 activity in HEK293T cells, yet because this phosphorylation was deemed critical for Snail1 function, we would expect to observe it in wild-type Snail1. The only phosphopeptide corresponding to serine 246 phosphorylation would coincide with phosphopeptide 1 after trypsin digestion (Figure 1D). As mentioned above, phosphopeptide 1 disappears in S11A mutant (Figure 2B), but was unaffected in S246A mutant (Supplemental Figure S2).

Also of note is that, with the exception of Snail1S92A mutation effecting phosphorylation at serine 82 (Figure 2D), the ablation of the various serines did not have significant effect on other phosphorylations, suggesting they occur independently of each other, although effects on global phosphorylation level cannot be discounted.

Overall, the present results indicate that Snail1 is phosphorylated in vivo at positions 11, 82, 92, 104, and 107 and that although other sites may be present, they are less frequently phosphorylated.

### Snail1 Is Phosphorylated by CK2 at Serine 92 and by PKA at Serine 11 In Vitro

To identify possible serine/threonine kinase candidates for the phosphorylated serines in Snail1 we carried out in silico analysis of Snail1 protein using NetphosK 1.0 server (http://www.cbs.dtu.dk/services/NetPhosK).

A probability score of 0.7 was given for PKA at serine 11 and 0.54 for CK2 at serine 92. For serines 104 and 107 the
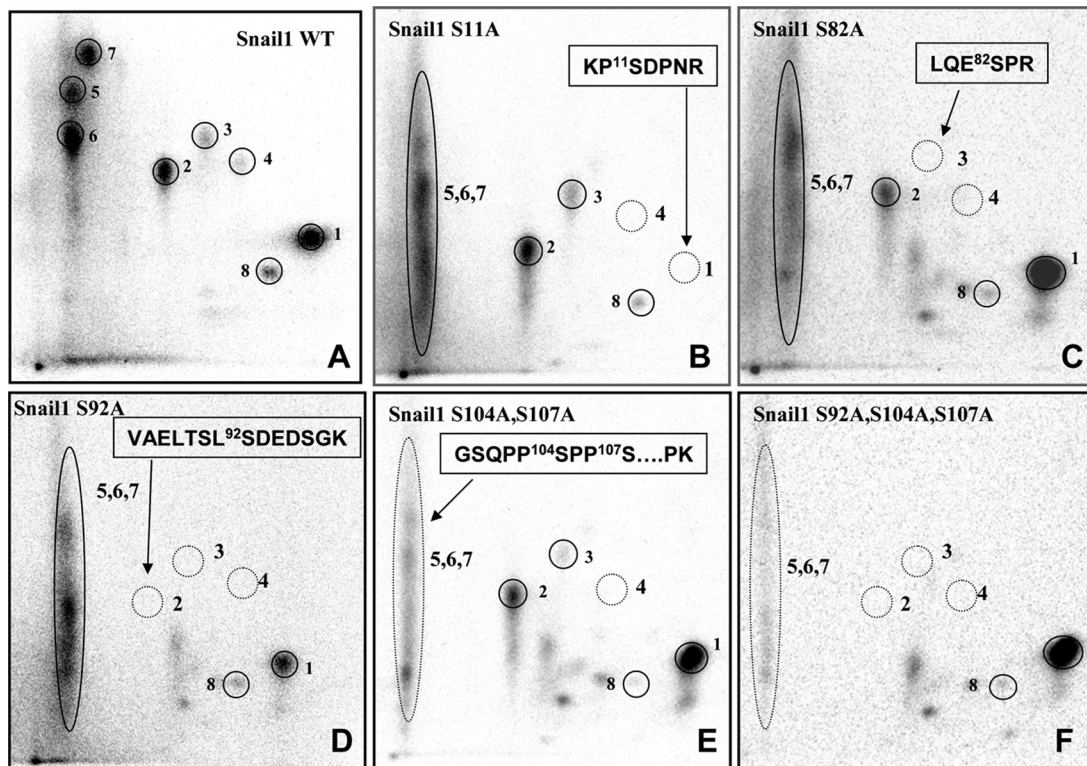
**Figure 2.** Phosphopeptide analyses of Snail1-HA mutants identify serine 11, 82, 92, 104, and 107 as the main in vivo phosphorylated residues. HEK293T cells transiently transfected with Snail1-HA wild-type (A) or Snail1-HA mutants (B–F) in the indicated serine residues were in vivo labeled with $^{32}$P-orthophosphate, and the immunoprecipitates obtained with anti-HA antibodies were subjected to tryptic digest and phosphopeptide analysis. Two-dimensional phosphopeptide mapping of (A) Snail1-HA wild type, (B) Snail1S11A mutant, (C) Snail1S82A mutant, (D) Snail1S92A mutant, (E) Snail1S104A/S107A double mutant, and (F) Snail1S92A/S104A/S107A triple mutant. The absence of phosphopeptide/s in each mutant is indicated by a dashed circle; the sequence of the corresponding phosphopeptides indicating the specific P-serine residue is also shown in each panel.

predicted kinase was GSK3$\beta$, and extensive investigations into the phosphorylation of these sites by this kinase have already been carried out (Zhou *et al.*, 2004; Yook *et al.*, 2005, 2006). There was no clear candidate for serine 82 phosphorylation and this will not be discussed further.

Therefore, we carried out in vitro phosphorylation reactions with PKA and CK2 on wild-type GST-Snail1 and the respective mutants, GST-Snail1S11A and GST-Snail1S92A. In the case of CK2, GST-Snail1 is readily phosphorylated by CK2 in vitro with relatively little phosphorylation of the GST-Snail1S92A mutant (Figure 3A). Phosphopeptide analysis identified a major spot from wild-type GST-Snail1 in the in vitro reaction of approximately the same mobility as that representing serine 92 phosphorylation in vivo (phosphopeptide 2; Figure 3B, left). In fact, Edmann's degradation of the main CK2 in vitro phosphopeptide rendered the same pattern as for in vivo phosphopeptide #2 (Figure 3C, cf. Figure 1C). Furthermore, this major spot was absent in the phosphopeptide mapping of Snail1S92A mutant (Figure 3B, right), confirming serine 92 as the main in vitro substrate of CK2.

In the case of PKA, a significant in vitro phosphorylation of wild-type GST-Snail1 was detected that was almost lacking in the GST-Snail1S11A mutant (Figure 4A). Furthermore, phosphopeptide analysis of wild-type GST-Snail1 in vitro phosphorylated by PKA identified a phosphorylated peptide of approximately the same mobility as that representing in vivo phosphorylation of serine 11 (phosphopeptide 1; Figure 4B, left) that was missing in the

GST-Snail1S11A mutant (Figure 4B, right). Therefore, these results support serine 11 as the main in vitro phosphorylation site of PKA.

### Snail1 Interacts with CK2α

Interestingly, a previous two-hybrid screening performed in our group to detect Snail1 interacting proteins identified several potential partners of Snail1, including LOXL2/3 proteins (Peinado *et al.*, 2005) and CK2α. Using the N-terminal regulatory domain of Snail1 (1–150) as bait, CK2α was confirmed as a positive interactor in the yeast system (Figure 5A). CK2 holoenzyme exists as a heterodimer consisting of two alpha and two beta subunits. CK2α is one of two possible alpha subunits, the other being CK2α′. To confirm the Snail1/CK2α interaction, pulldown assays were carried out using GST-Snail1 protein as bait and lysates from HEK293T cells transiently expressing CK2α-HA. We found that GST-Snail1 indeed interacts with CK2α-HA, whereas GST alone did not (Figure 5B). In vivo interaction was examined by coimmunoprecipitation analysis, after transient cotransfection of Flag-tagged Snail1 and CK2α-HA, but the results were negative, suggesting that the interaction in vivo is weak or transient in nature.

Overall, the evidence of in vivo and in vitro phosphorylation of Snail1 on the same residue and the yeast two-hybrid results strongly suggest that CK2 interacts with and may phosphorylate Snail1 at serine 92 in vivo.

**Figure 3.** Snail1 is phosphorylated in vitro by CK2 at serine 92. Recombinant GST-Snail1 and GST-Snail1S92A mutant were subjected to in vitro phosphorylation with CK2 holoenzyme. (A) Left, autoradiography showing phosphorylated bands from GST-Snail1 wild type (lane 3) and GST-Snail1S92A (lane 4); note the CK2 autophosphorylated bands detected in the absence (lane 1) and presence of GST alone (lane 2). Right, Coomassie blue stain of a parallel gel with equal amounts (10 $\mu$g) of GST-Snail1 wild type and GST-SnailS92A. (B) Two-dimensional phosphopeptide analysis corresponding to $^{32}$P-GST-Snail1 (left) and $^{32}$P-GST-Snail1S92A (right). For comparison, the in vivo phosphopeptide map of Snail1-HA is shown in an inset in the left panel. Note that the main phosphopeptide in GST-Snail1 showing the same mobility as in vivo phosphopeptide 2 (left, circle) is not present in the GST-Snail1S92A phosphopeptide mapping (right, dashed circle). (C) Edmann degradation analysis of phosphopeptide 2, isolated after in vitro CK2 phosphorylation of GST-Snail1; the sequence of corresponding peptide with phosphorylated serine 92 is indicated below.
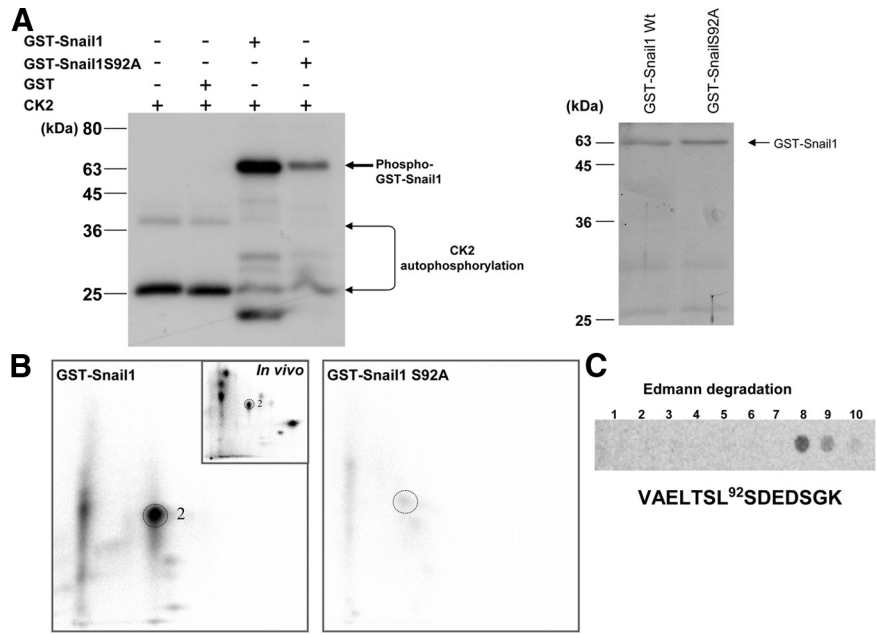


## Serine 11 and Serine 92 Are Required for Snail1-mediated Repression

To gain insight into the contribution of serine 11 and serine 92 in Snail1 functionality, the activity of the Snail1S11A and Snail1S92A mutants on the *E-cadherin* promoter was analyzed. Both mutants exhibited strongly decreased repressor activity (~20%) compared with the wild-type Snail1 protein on both the human (Figure 6A) or mouse *E-cadherin* promoter (Supplemental Figure S3A), indicating that serine 11 and serine 92 residues are required for an efficient Snail1 transcriptional repression on *E-cadherin*. Additional studies of other Snail1 target genes, such as *claudin-1* (Martinez-Estrada *et al.,* 2006), showed that the Snail1S11A and SnailS92A mutants also exhibited decreased repressor activity on *claudin-1* promoter, although a milder effect was observed for the Snail1S92A mutant activity compared with Snail1 wild type (Supplemental Figure S3B), suggesting an effective derepression action of the Snail1 mutants on additional target genes, apart from *E-cadherin*.

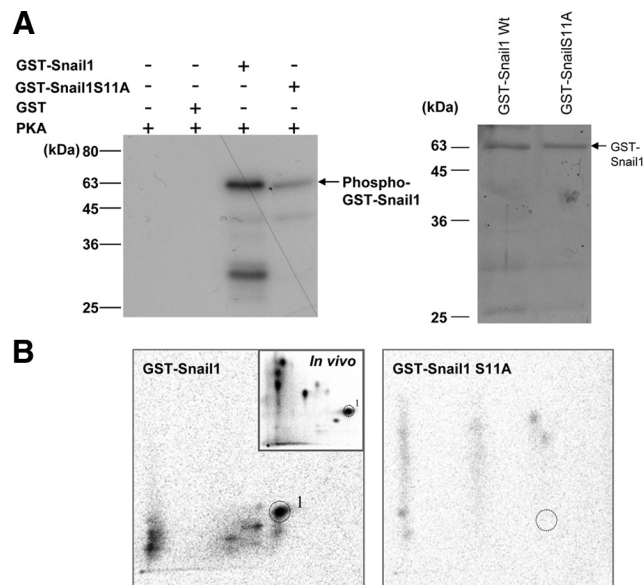Snail1 mediated *E-cadherin* repression depends on the SNAG domain and requires the recruitment of the mSin3A/



**Figure 4.** Snail1 is phosphorylated in vitro by PKA at serine 11. Recombinant GST-Snail1 and GST-Snail1S11A mutant were subjected to in vitro phosphorylation with PKA catalytic subunit. (A) Left, autoradiography showing phosphorylated bands from GST-Snail1 wild type (lane 3) and their virtual absence in GST-Snail1S11A (lane 4). Right, Coomassie blue stain of a parallel gel with equal amounts (10 $\mu$g) of GST-Snail1 wild type and GST-SnailS11A. (B) Two-dimensional phosphopeptide analysis corresponding to $^{32}$P-GST-Snail1 (left) and $^{32}$P-GST-Snail1S11A (right). For comparison, the in vivo phosphopeptide map of Snail1-HA is shown in an inset in the left panel. Note that the main phosphopeptide in GST-Snail1 showing the same mobility as in vivo phosphopeptide 1 (left, circle) is not present in the GST-Snail1S11A phosphopeptide mapping (right, dashed circle).
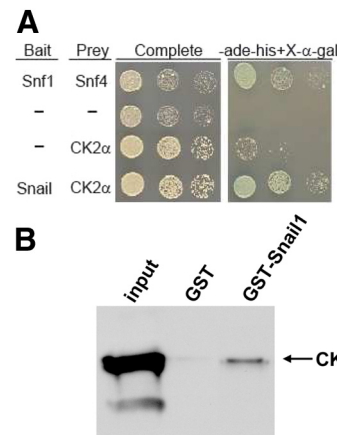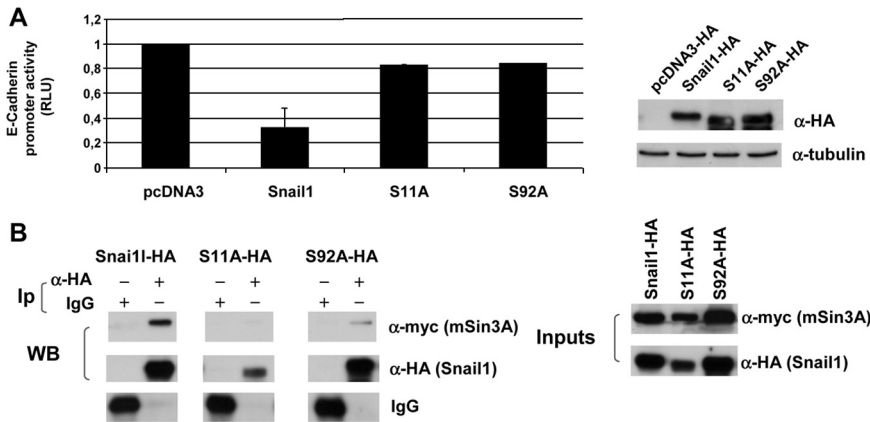


**Figure 5.** Snail1 interacts with CK2$\alpha$ in vivo and in vitro. (A) Two-hybrid analysis showing the specific in vivo interaction of Snail1 with CK2$\alpha$. (B) Pulldown analysis showing the interaction of recombinant GST-Snail1 (right) but not control GST (middle) with cell extracts obtained from HEK293T cells transiently transfected with CK2$\alpha$-HA. Input is shown in the left lane.

**Figure 6.** Phosphorylation of Snail1 at serine 11 and serine 92 is required for efficient repression of *E-cadherin* promoter and recruitment of mSin3A corepressor. (A) The repressor activity of Snail1-HA wild type and the indicated mutants on the human *E-cadherin* promoter was analyzed on HEK293T cells. Reporter assays were performed as described in *Material and Methods,* and relative luciferase units (RLU) normalized to the activity obtained in the presence of a void control pcDNA3 vector. Results show the mean of duplicate experiments, performed on quadruplicate samples; error bars, SD. Western blot showing similar expression levels of the different Snail1-HA constructs is shown on the right panel; α-tubulin was used as a loading control. (B) Coimmunoprecipitation analyses of Snail1-HA wild type and the indicated mutants with mSin3A-myc, after transient cotransfection in HEK293T cells. Top, immunoprecipitates were obtained with anti-HA affinity matrix or control IgG/Sepharose G beads (IgG), followed by Western blot with anti-myc and anti-HA to detect mSin3A and Snail1, respectively. Loading controls for IgG Ips are shown in the bottom panel; loading control IgG cannot be detected in the case of anti-HA immunoprecipitates, because they are retained inside the high-affinity anti-HA matrix. Inputs for transfected mSin3A-myc and Snail1-HA (wt or mutants) are shown in the right panels.

HDAC1/2 corepressor complex (Peinado *et al.,* 2004). Because serine 11 is located adjacent to the SNAG domain (Figure 1D), the interaction of Snail1S11A with the mSin3A corepressor was then studied by coimmunoprecipitation assays on HEK293T cells transiently transfected with Snail1-HA and mSin3A-myc. Results indicate that the Snail1S11A mutant has almost completely lost the interaction with mSin3A (Figure 6B, top middle panels). Interaction analysis of mSin3A corepressor with the Snail1S92A mutant also indicated a markedly reduced interaction with mSin3A compared with wild-type Snail1 (Figure 6B, top right panels). On the other hand, no significant changes in the nuclear localization of Snail1S11A or Snail1S92A mutants were observed (data not shown). These results indicate that phosphorylation of serine 11 or serine 92 does not affect Snail1 nucleo-cytoplasmic traffic machinery, yet positively influences the interaction of Snail1 with mSin3A corepressor, thus contributing to its transcriptional repression.

As the importance of specific serines in the SRD to Snail1 stability had been previously shown, we additionally examined the stability of Snail1S11A and Snail1S92A mutants, in comparison with wild-type Snail1, when transiently transfected in HEK293T cells. We found that the Snail1S92A mutation led to greatly increased stability compared with wild-type Snail1 (Figure 7, A and B), suggesting that phosphorylation at serine 92 forms part of the Snail1 degradation mechanism. Similar mutations at serine 96, 104, and 107 had previously been shown to increase Snail1 stability (Zhou *et al.,* 2004; Yook *et al.,* 2005) and, therefore, it appears that several phosphorylation sites inside the DB motif, or at its proximity, are involved in Snail1 degradation. In agreement with this, the double Snail1S104A/S107A mutant shows increased protein stability (Figure 7, C and D) and exhibits a repressive activity on the human *E-cadherin* promoter similar to that of Snail1 wild type in HEK293T cells (Supplemental Figure S4). In contrast to this behavior, the increased stability of the Snail1S92A mutant is not sufficient to maintain an efficient *E-cadherin* promoter repression (Figure 6A and Supplemental Figures S3–S5). Significantly, the phosphorylation mimicking Snail1S92E mutant rescues the repressor activity on *E-cadherin* promoter to levels similar to the Snail1 wild type (Supplemental Figure S5), indicating that electrostatic modification of serine 92 produced by phosphorylation is required for efficient Snail1-mediated re-

pression. Interestingly, the Snail1S11A mutant also showed a marked increased stability compared with wild-type Snail1 (Figure 7, C and D), despite its strongly decreased repressor activity (Figure 6A).

### Serine 11 and Serine 92 Are Required for Snail1 Functional Activity

To further explore whether the Snail1S11A and Snail1S92A mutations have any in vivo consequence we evaluated the competence of the Snail1 mutants to achieve EMT. To this end, MDCK cells were stably transfected with human Snail1-HA wild-type, Snail1S11A-HA, or Snail1S92A-HA versions. MDCK cells expressing Snail1-HA suffered EMT (80% of the clones) with complete loss of E-cadherin and increased expression and organization of vimentin (Figure 8, A, b, f, and j, and B) in agreement with previous observations (Peinado *et al.,* 2005). In contrast, MDCK cells expressing the Snail1S11A-HA mutant exhibited an unaltered epithelial phenotype (75% of the clones) similar to that of the mock-control cells (Figure 8A, cf. c and d with a) and maintain the expression of E-cadherin (Figure 8B) organized in cell–cell junctions (Figure 8A, cf. g and h, with e) and basal vimentin levels (Figure 8A, cf. k and l with i). Importantly, the majority of MCDK-Snail1S11A-HA clones express the mutant Snail1S11A protein to levels similar to those of Snail1-HA wild type present in MDCK-Snail1 suffering EMT (Figure 8C). Strikingly, repeated attempts to stably express the Snail1S92A-HA mutant were unsuccessful or resulted in a very low number of stable colonies, suggesting that mutation of serine 92 has a deleterious effect on survival of MDCK cells. Indeed, analysis of the isolated clones indicated that although most of them maintain the epithelial phenotype with absence of EMT features (Supplemental Figure S6, A and B), they express almost undetectable levels of Snail1-S92A-HA protein even lower of basal endogenous Snail1 (Supplemental Figure S6C). The basal nonfunctional level of endogenous Snail1 detected in control MDCK-CMV cells is in agreement with our previous observations (Peinado *et al.,* 2005). These results reinforce the functional requirement of intact S11 and S92 residues for Snail1 function in EMT and cell survival, respectively.

Taken together, these results strongly suggest that phosphorylation of serine 92 and serine 11 positively regulates
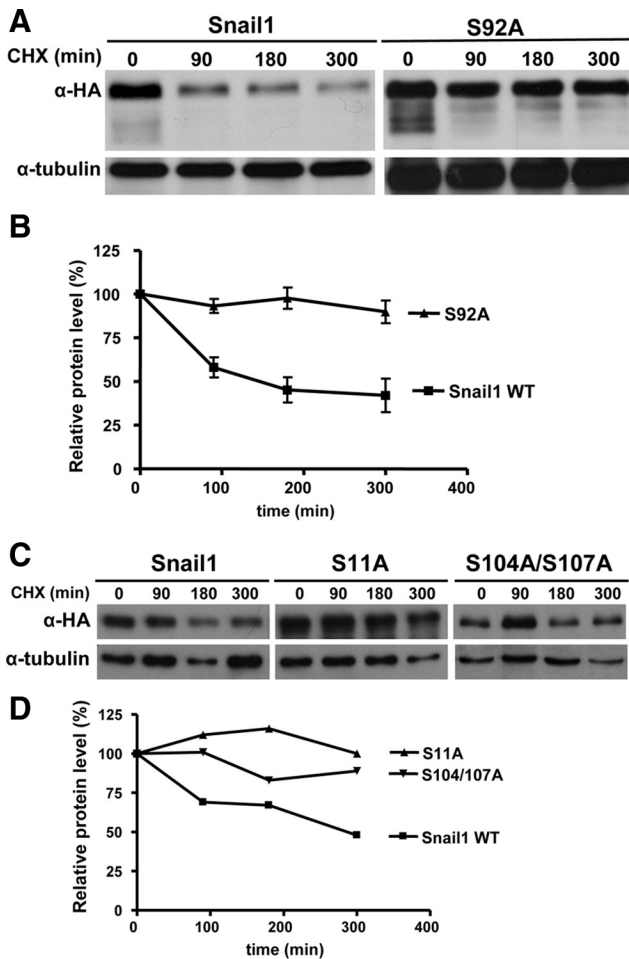
**Figure 7.** Serine to alanine mutation in serine 11, 92, and 104/107 increases Snail1 stability. (A and C) The stability of Snail1-HA and the indicated Snail1-HA mutants in HEK293T cells was determined by incubation in the presence of the translational inhibitor cycloheximide (CHX) for the indicated time periods. Snail1-HA levels were determined at each time point by Western blot analysis with anti-HA antibodies; α-tubulin was used as a loading control. (B and D) Densitometric quantification of the relative amounts of Snail1-HA and indicated mutants allowed determination of the differential stability of the various mutants compared with Snail1-HA wild type. Results show the mean of three different experiments; error bars, SD (B) and a representative experiment (D) corresponding to the quantification of the membranes shown in C.

Snail1 functionality and point to the participation of CK2 and PKA, respectively, in those phosphorylation events.

## DISCUSSION

The role of Snail1 in development and tumor invasion is well established and understanding the regulatory mechanisms controlling Snail1 functionality will facilitate the development of new strategies and targets for cancer treatment. To date, several studies had examined the control of Snail1 through phosphorylation, supporting the action of negative (GSK3β) and positive (PAK1) kinase players (Zhou et al., 2004; Yang et al., 2005; Yook et al., 2005). Recently, identification of the small C-terminal domain phosphatase (SCP) as responsible for dephosphorylation of Snail1-GSK3β phosphorylated has added a new level of regulation (Wu et
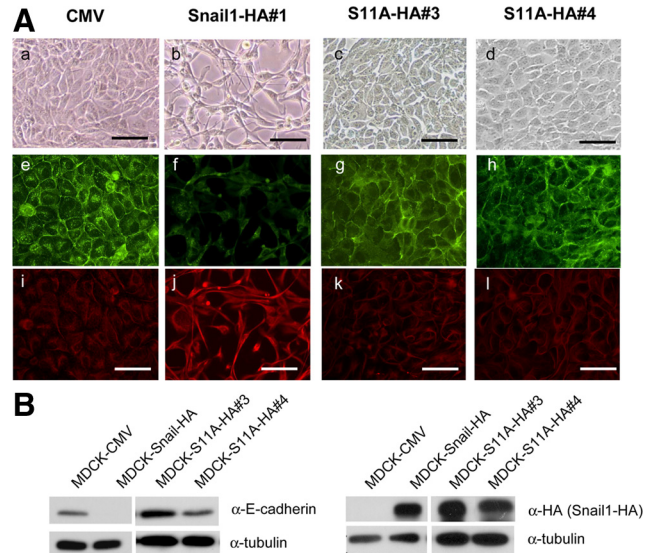


**Figure 8.** Serine 11 is required for Snail1 induction of EMT. Snail-1-HA wild type and Snail1-S11A-HA mutant were stably transfected into MDCK cells, and selected clones were analyzed for phenotype and EMT markers. (A) Phenotypic characterization of one representative Snail1-HA clone (1) and two representative Snail1-S11A clones, S11A3 and S11A4 compared with control MDCK-CMV (CMV) cells. (a–d) Phase-contrast images; (e–l) immunofluorescence staining for E-cadherin (green; e–h) and vimentin (red; i–l). Bar, 200 μm. (B) Western blot analysis of the indicated clones for E-cadherin (left) and Snail1-HA (right) detection using anti-HA antibodies in the later case. α-Tubulin was used as loading control. Similar results were obtained for all isolated clones.

al., 2009b). An alternative mechanism for Snail1 stabilization by TNF-α/NF-κB pathway independent of GSK3β phosphorylation has been recently described (Wu et al., 2009a), indicating the existence of several pathways to control Snail1 stability in response to different cues. However, in none of these studies was there a detailed analysis of in vivo Snail1 phosphorylation and its influence in Snail1 repressor and functional activity. Here, we presented a detailed analysis of human Snail1 in vivo phosphorylation. Phosphopeptide and mutational analysis demonstrate that Snail1 serines 11, 82, 92, 104, and 107 were phosphorylated in vivo. Importantly, phosphorylations of S11 and S92 are independently required for Snail1 repressor activity of E-cadherin promoter and for efficient recruitment of the mSin3A corepressor. Furthermore, intact serine 11 and serine 92 are required for in vivo Snail1 function in induction of EMT and/or cell survival, respectively.

It had been initially shown, through in vivo phosphoamino acid analysis that the majority of Snail1 phosphorylations occurred on serine residues (Domínguez et al., 2003). Furthermore, those previous studies demonstrated a marked reduction in phosphorylation of Snail1 mutants generated either by mutating all serines to alanine between residues 82-123 or by deleting this region entirely (Domínguez et al., 2003). Our present results indicate that this is due to the lack of phosphorylation at serines 82, 92, 104, and 107, and the remaining phosphorylation observed in those mutants would be attributed to serine 11. Two other investigations have previously examined Snail1 SRD phosphorylation (Zhou et al., 2004; Yook et al., 2005), demonstrating a role for GSK3β in SRD phosphorylation and regulation of Snail1 stability, through slightly different models.

Notably, Yook *et al.* (2005) found serines 104 and 107 to be the only double mutant with significant effect on Snail1 stability, emphasizing the importance of these two residues. In agreement with those previous observations, we found both serines 104 and 107 to be phosphorylated together in vivo. Zhou and colleagues proposed a slightly different model where GSK3$\beta$ initially phosphorylates Snail1 in the nucleus at serines 119, 115, 111, and 107, promoting its nuclear export to the cytoplasm where GSK3$\beta$ further phosphorylates the DB serines (S96 and S100), eliciting ubiquitination and degradation. However, we observed serines 104 and 107 phosphorylated together without detectable phosphorylation of serines 111, 115, and 119. Furthermore, mutations of Snail1 at serines 111, 115, and 119 did not result in obvious changes in the in vivo phosphorylation pattern or abrogation of the phosphopeptides corresponding to S104 and S107, suggesting that these are not "priming" phosphorylations (data not shown). Overall, our in vivo data tend to support the model originally proposed by Yook *et al.* (2005), favoring that GSK3$\beta$ probably phosphorylates serines 104 and 107 and then 96 and 100 to promote degradation. However, we should not completely discount the possibility of phosphorylations at serines 111, 115, and 119 because the resolution of the larger peptide species containing the SRD was poor and sequencing may have missed phosphorylations so distant from the N-termini of the peptide. Surprisingly, we could not detect in vivo phosphorylation at serines 96 and 100, although we suspect that the ubiquitination and degradation of this Snail1 species prevented observance of these phosphorylations.

The serine at position 82 appears more cryptic and is only weakly phosphorylated relative to other serines in Snail1. In silico analysis did not reveal any likely kinase candidates although GSK3$\beta$ and p38MAPK had the highest probability scores of 0.48. Despite this, phosphorylation at serine 82 appears to be influenced by that on serine 92, because it completely disappears in mutant Snail1S92A, perhaps by promoting a conformational change. The functional significance of serine 82 phosphorylation remains to be investigated.

Also of interest, was the lack of detection in our analysis of in vivo phosphorylation at serine 246 previously speculated to be critical for Snail1 function (Yang *et al.*, 2005). In our hands, mutation at this site resulted in no effect on Snail1's phosphorylation pattern, cellular localization, or function (Supplemental Figures S1 and S2; data not shown). It may be that the effects observed previously in this mutant are due to secondary effects present in particular cellular contexts, due to changes in zinc finger binding or on nuclear import sequences lying nearby (Mingot *et al.*, 2009).

Our present study provides evidence for new regulatory phosphorylation events in Snail1 at serine 92 and at serine 11 with consequences in Snail1 stability and, more importantly, in Snail1-mediated repression and functional activity. Interestingly, phosphorylation of serine 92 does not appear to prime or stimulate phosphorylation in the SRD region, because no change in the phosphorylation pattern in this region was observed in the Snail1S92A mutant. However, we observed that, despite its increased stability, the Snail1S92A mutant has strongly decreased repressor activity on the *E-cadherin* promoter relative to Snail1 wild type. Importantly, this was associated to a marked decreased interaction with mSin3A corepressor. These observations indicate that phosphorylation at serine 92 positively regulates Snail1 transcriptional repression by a mechanism dependent on efficient recruitment of mSin3A corepressor.

We also observed phosphorylation at serine 11, adjacent to the SNAG domain known to be critical for Snail1 repressive action and interaction with corepressors (Hemavathy *et al.*, 2002; Peinado *et al.*, 2004). Ablation of S11 phosphorylation, despite inducing increased stability, strongly attenuated Snail1 repression on *E-cadherin* and *claudin-1* promoters, suggesting that serine 11 phosphorylation is necessary for correct interaction with corepressors. Indeed almost complete abrogation of interaction with mSin3A was detected in the Snail1S11A mutant. Mutation of this site did not result in any change in subcellular localization despite its proximity to lysines (K9, K16) identified as part of a nuclear import signal (Ko *et al.*, 2007), although recent studies also indicate the participation of residues in the zinc finger region for efficient Snail1 nuclear import (Mingot *et al.*, 2009). Interestingly, the in vitro phosphorylation studies identified serine 92 and serine 11 as the main phosphorylated substrates of CK2 and PKA, respectively, suggesting that both kinases may be involved in Snail1 regulation in vivo by directly modulating Snail1-mSin3A interaction.

The direct implication of serine 11 in Snail1 activity has been demonstrated in functional transfection studies, because mutation of serine 11 abrogates the EMT inducing activity of Snail1, indicating that intact serine 11 is required for Snail1 to drive the EMT program, affecting not only *E-cadherin* repression but the regulation of other Snail1 target genes, like *claudin-1*. Mutation of serine 92 in Snail1 also results in abrogation of the EMT program and, strikingly, in cell lethality, reinforcing the functional requirement of serine 92 for EMT and additional Snail1 functions as cell survival (Vega *et al.*, 2004), although further studies are required to characterize the involvement of serine 92 in Snail1-mediated regulation of cell survival.

The results presented here strongly support that phosphorylation of Snail1 at serine 11 and serine 92, likely mediated by PKA and CK2, respectively, emerge as new positive regulatory pathways of Snail1 repressor activity both influencing mSin3A corepressor recruitment and functional activity. In this context, it is interesting to note that $\beta$-catenin is also regulated by CK2 and PKA phosphorylation, both directly and through its interaction with APC (Song *et al.*, 2003; Hildesheim *et al.*, 2005; Taurin *et al.*, 2006). Regulation of the tumor suppressor PML by CK2 has also been shown (Scaglioni *et al.*, 2006; Stehmeier and Muller, 2009). The positive regulation of Snail1 function by CK2 proposed here, provides new mechanistic aspects to support the participation of this kinase in tumorigenesis.

Taken together, the present results reinforce the existence of a complex regulatory network in Snail1 posttranslational regulation involving activating and inhibitory phosphorylation mechanisms and putting into the stage new players as serines 11 and 92 and, potentially, CK2 and PKA kinases. These observations, together with recently reported alternative mechanisms for Snail1 stabilization (Evdokimova *et al.*, 2009; Wu *et al.*, 2009a), provide potential novel targets to influence Snail1 function in tumor progression.

## REFERENCES

Batlle, E., Sancho, E., Franci, C., Domínguez, D., Monfar, M., Baulida, J., and Garcia De Herreros, A. (2000). The transcription factor Snail is a repressor of E-cadherin gene expression in epithelial tumour cells. Nat. Cell Biol. *2*, 84–89.

Barrallo-Gimeno, A., and Nieto, M. (2005). The Snail genes as inducers of cell movement and survival: implications in development and cancer. Development *132*, 3151–3161.

Boley, W. J., Van Der Geer, P., and Hunter, T. (1991). Phosphopeptide mapping and phosphoamino acid analysis by two-dimensional separation on thin-layer cellulose plates, Methods Enzymol. *201*, 110–149.

Cano, A., Perez-Moreno, M. A., Rodrigo, I., Locascio, A., Blanco, M. J., del Barrio, M. G., Portillo, F., and Nieto, M. A. (2000). The transcription factor Snail controls epithelial-mesenchymal transitions by repressing E-cadherin expression. Nat. Cell Biol. *2*, 76–83.

Carver, E. A., Jiang, R., Lan, Y., Oram, K. F., and Gridley, T. (2001). The mouse snail gene encodes a key regulator of the epithelial-mesenchymal transition. Mol. Cell. Biol. *21*, 8184–8188.

Domínguez, D., Montserrat-Sentís, B., Virgós-Soler, A., Guaita, S., Grueso, J., Porta, M., Puig, I., Baulida, J., Francí, C., and García de Herreros, A. (2003). Phosphorylation regulates the subcellular location and activity of the snail transcriptional repressor. Mol. Cell. Biol. *3*, 5078–5089.

Evdokimova, V., *et al.* (2009). Translational activation of snail1 and other developmentally regulated transcription factors by YB-1 promotes an epithelial-mesenchymal transition. Cancer Cell *5*, 402–415.

Francí, C., *et al.* (2006). Expression of Snail protein in tumor-stroma interface. Oncogene *25*, 5134–5144.

Francí, C., Gallén, M., Alameda, F., Baró, T., Iglesias, M., Virtanen, I., and García de Herreros, A. (2009). Snail1 protein in the stroma as a new putative prognosis marker for colon tumours. PLoS ONE *4*(5), e5595. doi:10.1371/journal.pone. 0005595.

Gupta, G. P., and Massagué, J. (2006). Cancer metastasis: building a framework. Cell *127*, 679–695.

Hemavathy, K., Guru, S. C., Harris, J., Chen, J. D., and Ip, Y. T. (2000). Human Slug is a repressor that localizes to sites of active transcription. Mol. Cell. Biol. *20*, 5087–5095.

Hildesheim, J., Salvador, J. M., Hollander, M. C., and Fornace, A. J., Jr. (2005). Casein kinase 2- and protein kinase A-regulated adenomatous polyposis coli and beta-catenin cellular localization is dependent on p38 MAPK. J. Biol. Chem. *280*, 17221–17226.

Ko, H., Kim, H. S., Kim, N. H., Lee, S. H., Kim, K. H., Hong, S. H., and Yook, J. I. (2007). Nuclear localization signals of the E-cadherin transcriptional repressor Snail. Cells Tissues Organs *185*, 66–72.

Manzanares, M., Locascio, A., and Nieto, M. A. (2001). The increasing complexity of the Snail gene superfamily in metazoan evolution. Trends Genet. *17*, 78–81.

Martinez-Estrada, O. M., Cullerés, A., Soriano, F. X., Peinado, H., Bolós, V., Martinez, F. O., Reina, M., Cano, A., Fabre, M., and Vilaró, S (2006). The transcription factors Slug and Snail act as repressors of Claudin-1 expression in epithelial cells. Biochem J. *394*, 449–457.

Mingot, J. M., Vega, S., Maestro, B., Sanz, J. M., and Nieto, M. A. (2009). Characterization of Snail nuclear import pathways as representatives of C2H2 zinc finger transcription factors. J. Cell Sci. *122*, 1452–1460.

Moreno-Bueno, G., Portillo, F., and Cano, A. (2008). Transcriptional regulation of cell polarity in EMT and cancer. Oncogene *27*, 6958–6969.

Nelson, W. J., and Nusse, R. (2004). Convergence of Wnt, beta-catenin, and cadherin pathways. Science *303*, 1483–1487.

Nieto, M. A. (2002). The snail superfamily of zinc-finger transcription factors. Nat. Rev. Mol. Cell Biol. *3*, 155–166.

Peinado, H., Ballestar, E., Esteller, M., and Cano, A. (2004). Snai1 mediates E-cadherin repression by recruitment of the Sin3A/histone deacetylase 1 (HDAC1)/HDAC2 complex. Mol. Cell. Biol. *24*, 306–319.

Peinado, H., Iglesias-de la Cruz, M. C., Olmeda, D., Csiszar, K., Fong, K. S., Vega, S., Nieto, M. A., Cano, A., and Portillo, F. (2005). A molecular role for lysyl oxidase-like 2 enzyme in snail regulation and tumor progression. EMBO J. *24*, 3446–3458.

Peinado, H., Olmeda, D., and Cano, A. (2007). Snail, ZEB, and bHLH factors in tumour progression: an alliance against the epithelial phenotype? Nat. Rev. Cancer *7*, 415–428.

Scaglioni. P. P., Yung, T. M., Cai. L. F., Erdjument-Bromage, H., Kaufman, A. J., Singh, B., Teruya-Feldstein, J., Tempst, P., and Pandolfi, P. P. (2006). A CK2-dependent mechanism for degradation of the PML tumor suppressor. Cell *126*, 269–283.

Sefton, M., Sánchez, S., and Nieto, M. A. (1998). Conserved and divergent roles for members of the Snail family of transcription factors in the chick and mouse embryo. Development *125*, 3111–3121.

Song, D. H., Dominguez, I., Mizuno, J., Kaut, M., Mohr, S. C., and Seldin, D. C. (2003). CK2 phosphorylation of the armadillo repeat region of beta-catenin potentiates Wnt signaling. J. Biol. Chem. *278*, 4018–4025.

Stehmeier, P., and Muller, S. (2009). Phospho-regulated SUMO interaction modules connect the SUMO system to CK2 signaling. Mol. Cell *33*, 400–409.

Taurin, S., Sandbo, N., Qin, Y., Browning, D., and Dulin, N. O. (2006). Phosphorylation of beta-catenin by cyclic AMP-dependent protein kinase. J. Biol. Chem. *281*, 9971–9976.

Thiery, J. P. (2002). Epithelial-mesenchymal transitions in tumour progression. Nat. Rev. Cancer *2*, 442–454.

Van Der Geer, P., and Hunter, T. (1994). Phosphopeptide mapping and phosphoamino acid analysis by electrophoresis and chromatography on thin-layer cellulose plates. Electrophoresis *15*, 544–554.

Vega, S., Morales, A. V., Ocaña, O. H., Valdés, F., Fabregat, I., and Nieto, M. A. (2004). Snail blocks the cell cycle and confers resistance to cell death. Genes Dev. *18*, 1131–1143.

Vernon, A. E., and Labonne, C. (2006). Slug stability is dynamically regulated during neural crest development by the F-box protein Ppa. Development *133*, 3359–3370.

Wu, Y., Deng, J., Rychahou, P. G., Qiu, S., Evers, B. M., and Zhou, B. P. (2009a). Stabilization of snail by NF-kappaB is required for inflammation-induced cell migration and invasion. Cancer Cell *15*, 416–428.

Wu, Y., Evers, B. M., and Zhou, B. P. (2009b). Small C-terminal domain phosphatase enhances snail activity through dephosphorylation. J. Biol. Chem. *284*, 640–648.

Yang, Z., Rayala, S., Nguyen, D., Vadlamudi, R. K., Chen, S., and Kumar, R. (2005). Pak1 phosphorylation of snail, a master regulator of epithelial-to-mesenchyme transition, modulates snail's subcellular localization and functions. Cancer Res. *65*, 3179–3184.

Yang, J., and Weinberg, R. A. (2008). Epithelial-mesenchymal transition: at the crossroads of development and tumor metastasis. Dev. Cell *14*, 818–829.

Yook, J. I., Li, X. Y., Ota, I., Fearon, E. R., and Weiss, S. J. (2005). Wnt-dependent regulation of the E-cadherin repressor snail. J. Biol. Chem. *280*, 11740–11748.

Yook, J. I., *et al.* (2006). A Wnt-Axin2-GSK3beta cascade regulates Snail1 activity in breast cancer cells. Nat. Cell Biol. *8*, 1398–1406.

Zheng. L., Baumann, U., and Reymond, J. L. (2004). An efficient one-step site-directed and site-saturation mutagenesis protocol. Nucleic Acid Res. *2*, e115.

Zhou, B. P., Deng, J., Xia, W., Xu, J., Li, Y. M., Gunduz, M., and Hung, M. C. (2004). Dual regulation of Snail by GSK-3beta-mediated phosphorylation in control of epithelial-mesenchymal transition. Nat. Cell Biol. *6*, 931–940.